Atmos. Meas. Tech., 2, 465–477, 2009
www.atmos-meas-tech.net/2/465/2009/

Atmospheric Measurement Techniques

A flow-tube based laser-induced fluorescence instrument to measure OH reactivity in the troposphere

T. Ingham[1,3], A. Goddard[1], L. K. Whalley[1,3], K. L. Furneaux[1,†], P. M. Edwards[1], C. P. Seal[1], D. E. Self[1], G. P. Johnson[1], K. A. Read[2,4], J. D. Lee[2,4], and D. E. Heard[1,3]

[1]School of Chemistry, University of Leeds, Leeds, LS2 9JT, UK
[2]Department of Chemistry, University of York, York, YO10 5DD, UK
[3]National Centre for Atmospheric Science (NCAS), University of Leeds, Leeds, LS2 9JT, UK
[4]National Centre for Atmospheric Science (NCAS), University of York, York, YO10 5DD, UK
[†]deceased, 28 July 2009

Received: 19 January 2009 – Published in Atmos. Meas. Tech. Discuss.: 2 March 2009
Revised: 9 July 2009 – Accepted: 10 July 2009 – Published: 31 August 2009

Abstract. A field instrument utilising the artificial generation of OH radicals in a sliding injector flow-tube reactor with detection by laser-induced fluorescence spectroscopy has been developed to measure the rate of decay of OH by reaction with its atmospheric sinks. The OH reactivity instrument has been calibrated using known concentrations of CO, NO_2 and single hydrocarbons in a flow of zero air, and the impact of recycling of OH via the reaction HO_2+NO→OH+NO_2 on the measured OH reactivity has been quantified. As well as a detailed description of the apparatus, the capabilities of the new instrument are illustrated using representative results from deployment in the semi-polluted marine boundary layer at the Weybourne Atmospheric Observatory, UK, and in a tropical rainforest at the Bukit Atur Global Atmospheric Watch station, Danum Valley, Borneo.

1 Introduction

The highly reactive hydroxyl radical, OH, is the major oxidising species in the troposphere, and governs the atmospheric lifetimes of most trace species of biogenic and anthropogenic origin. OH initiates oxidative radical chain reactions which remove primary pollutants and greenhouse gases such as CO, methane, non-methane volatile organic compounds (VOCs), NO_x, and SO_2. These processes convert these compounds into secondary pollutants such as O_3, peroxy acetyl nitrates, and sulphuric acid which are potentially harmful. For example, the oxidation of a hydrocarbon (RH) proceeds via the following mechanism:

$$OH + RH \rightarrow R + H_2O \quad \text{(R1)}$$

$$R + O_2 + M \rightarrow RO_2 + M \quad \text{(R2)}$$

$$RO_2 + NO \rightarrow RO + NO_2 \quad \text{(R3)}$$

$$RO + O_2 \rightarrow HO_2 + \text{carbonyl} \quad \text{(R4)}$$

$$HO_2 + NO \rightarrow OH + NO_2 \quad \text{(R5)}$$

$$NO_2 + h\nu \rightarrow NO + O(^3P) \quad \text{(R6)}$$

$$O(^3P) + O_2 + M \rightarrow O_3 + M \quad \text{(R7)}$$

where R is an organic group and M is a third body reactant (O_2 or N_2). Products of OH oxidation, for example H_2SO_4 and oxygenated VOCs, have low vapour pressures and participate in processes leading to the formation of new particles and secondary organic aerosol. Under most conditions, the dominant (or "primary") tropospheric source of OH radicals is the photolysis of O_3 to yield $O(^1D)$ atoms, the majority of which are collisionally quenched to the $O(^3P)$ ground state by O_2 or N_2 reforming O_3 by reaction (7), with the remainder reacting with H_2O to produce two OH radicals:

$$O_3 + h\nu \rightarrow O(^1D) + O_2 (\lambda < 340\,\text{nm}) \quad \text{(R8)}$$

$$O(^1D) + H_2O \rightarrow 2\,OH \quad \text{(R9)}$$

Secondary OH sources include the conversion of HO_2 to OH by reaction (5), the photolysis of carbonyls, peroxides and HONO, and alkene ozonolysis. Novel production mechanisms of OH, for example the reaction of electronically excited NO_2 with water vapour, have recently been suggested

Correspondence to: D. E. Heard
(d.e.heard@leeds.ac.uk)

by Li et al. (2008). The overall rate of OH production (P_{OH}) is given by:

$$P_{OH}=2f[O_3]j(O^1D)+k_5[HO_2][NO]+j_X[X] \quad (1)$$
$$+\text{rate of other production steps}$$

where $j(O^1D)$ is the rate of O_3 photolysis to generate $O(^1D)$ atoms and f is the fraction of $O(^1D)$ atoms which react with water vapour to produce OH rather than undergoing collisional quenching ($f \sim 0.1$ under normal tropospheric conditions).

The high reactivity of the OH radical ensures that it reacts on a much faster timescale than other stable compounds involved in its production and loss, enabling the steady-state approximation to be made, and allowing the effects of air mass transport in determining the concentration of local [OH] to be ignored. At steady-state the production and loss of OH is given by:

$$d[OH]/dt = P_{OH}-k'[OH]=P_{OH}-\frac{[OH]}{\tau_{OH}}=0$$
$$[OH]=\frac{P_{OH}}{k'}=P_{OH}\ \tau_{\ OH} \quad (2)$$

where $k'[OH]$ represents the total pseudo-first-order loss rate of OH radicals due to reaction with trace gases, or the OH reactivity, which is the inverse of the OH chemical lifetime, τ_{OH}. Field measurement of k' can be compared with a value calculated using the concentration of co-measured OH sinks and relevant kinetic data, in order to gauge the fraction of OH sinks that are not being measured. Furthermore, equipped with a knowledge of [OH], the value of k' can be used to obtain $P(OH)$, the rate of production of OH, and through comparison with the calculated production rate via measurement of $2f[O_3]j(O^1D)$ and other terms on the right hand side of Eq. (1), the fraction of the OH production rate that is not being measured can be quantified.

[OH] is unaffected by transport processes, depending only on the in situ local chemical environment and solar irradiance. Hence it is an ideal target species to test the accuracy of tropospheric chemical mechanisms via comparison of measured [OH] with predictions of zero-dimensional models constrained by supporting measurements of the longer-lived OH co-reactant trace gas concentrations, and photolysis rates, that define its rate of production and loss. Tropospheric measurements of OH concentrations have been made in various environments for about two decades (Heard and Pilling, 2003, and references therein) together with supporting measurements, and, whilst the measured/modelled agreement has in general improved, there remain discrepancies (Heard and Pilling, 2003; Carslaw et al., 1999; McKeen et al., 1997; Bell et al., 2003). A commonly suggested hypothesis for model over-prediction of [OH] is an incomplete suite of supporting measurements of trace gas compounds that act as OH sinks (Heard and Pilling, 2003). The use of two-dimensional chromatography indicated that significant levels of hydrocarbons are not measured by standard equipment used in many field studies (Lewis et al., 2000). A recent example of significant model under-prediction occurred for conditions above a tropical rainforest in Suriname following the measurement of elevated OH concentrations. The recycling of OH, postulated as being from reactions of HO_2 radicals with organic peroxy radicals originating from the oxidation of isoprene or other biogenic species, is required to match measurements (Lelieveld et al., 2008). However, one must be careful in the quest for perfect agreement between field measured and modelled [OH], as both OH sources and sinks may remain unmeasured, and hence both $P(OH)$ and k' underestimated. Cancellation of errors due to missing sources and sinks in Eq. (2) may lead to good agreement for the wrong reasons.

Field measurements of the OH reactivity, k', were first reported in 2001 and have now been made in diverse environments. The OH reactivity was measured during the Southern Oxidants Study (SOS, Nashville, Tennessee) and found to be, at times, almost double that calculated from the supporting measurements of co-reactants, but on average over the campaign was a factor of ca. 1.33 higher, with the OH reactivity displaying a small diurnal variation (Kovacs and Brune, 2001; Kovacs et al., 2003; Martinez et al., 2003). The OH reactivity was measured in suburban and urban Tokyo and found to be a factor of ca. 1.3 higher than calculated in summer, spring, and winter, but in winter no significant difference was observable (Sadanaga et al., 2004b; Sadanaga et al., 2005; Yoshino et al., 2006). As part of the PM2.5 Technology Assessment and Characterisation Study-New York (PMTACS-NY, summer 2001) (Ren et al., 2003) and a second New York study held in Winter (Ren et al., 2006a) the measured reactivity agreed to within 10% of the calculated reactivity in the urban atmosphere of New York City in the summer campaign, but there was a much larger missing reactivity (30–40%) at rush hour in the morning and evening of the winter campaign. However, during the Mexico City Metropolitan Area study (MCMA, Mexico City, 2003) early morning rush hour OH loss rates of $120\,s^{-1}$ (mean) were observed (Shirley et al., 2006), a factor of ca. 5 higher than those observed for the rush hour in New York City. Several field campaigns, including those in clean environments, have shown that the OH reactivity is dominated by oxygenated VOCs, for example carbonyl species and alcohols, rather than hydrocarbons (Lewis et al., 2005; Emmerson et al., 2007), species which are more difficult to measure and not routinely quantified. Measurements at a remote, clean site at Whiteface Mountain (upper New York State) showed only a slight diurnal variation with an average reactivity of $5.6\,s^{-1}$ (Ren et al., 2006b) similar to that observed at another rural site at Rock Springs, Pennsylvania (Ren et al., 2005). Very recently, the first airborne measurements of OH reactivity were made (Mao et al., 2009).

There have been two measurements of OH reactivity in two contrasting forested environments. In 2000, k' was measured in the great Lakes region of northern Michigan (USA)

(45.5° N) in a mixed hardwood forest (Di Carlo et al., 2004). The "missing" reactivity, defined as the difference between the measured and calculated reactivity (using co-measured isoprene and other terpene and biogenic VOCs (BVOCs)) was found to increase exponentially with temperature, similar to the rates of emission of isoprene and other terpenes. The study concluded that the missing OH reactivity orginates from unknown reactive BVOCs. OH reactivities, k', as high as $72\,s^{-1}$ were measured in the tropical rainforest of Suriname (5° N) during 2 h in 2005, being a factor of 3 higher than the calculated reactivity using co-measurements of isoprene, its oxidation products and other VOCs (Sinha et al., 2008). Whilst there are studies where the agreement between measured and calculated OH reactivity is fairly good, several studies show missing reactivity to various extents, and there remains a need to characterise the OH reactivity in a wider range of environments.

In this paper, a description is given of an instrument to measure the OH reactivity, k'. Experiments to characterise and calibrate the instrument are described, and some illustrative measurements are presented for a semi-polluted site in Norfolk, UK, and a tropical rainforest in Borneo, to demonstrate the capabilities of the instrument.

2 Experimental

Three methods are described in the literature for the measurement of OH reactivity, all of which are perturbation techniques involving the photolytic production of above ambient levels of OH. Two of the methods use laser-induced fluorescence spectroscopy (LIF) to measure the subsequent relaxation of the OH concentration under pseudo-first-order conditions. In the first of these to be developed (Kovacs and Brune, 2001), a mercury lamp photolyses water vapour at 185 nm within a sliding injector to continuously produce OH (and HO_2 radicals) which are injected into a flow tube:

$$H_2O + hv(185\,nm) \rightarrow OH + H \quad \text{(R10)}$$

$$H + O_2 + M \rightarrow HO_2 + M \quad \text{(R11)}$$

The subsequent decay of OH radicals is recorded as the flow tube injector is retracted to increase the distance from production to sampling, and the average flow velocity in the flow tube is used to convert injector distance (s) to reaction time (t) (Kovacs and Brune, 2001; Mao et al., 2009).

In the second LIF method, a 266 nm pulsed laser (10 Hz pulse repetition frequency) is used to photolyse O_3 within the ambient air sample, the $O(^1D)$ produced reacting with ambient water vapour via reaction (Eq. 4) to produce two OH radicals, without initially generating any HO_2 radicals. In this pulsed pump-probe method, the OH decay is observed directly by time-resolved LIF (Sadanaga et al., 2004a). Ambient air is sampled at ca. 20 SLM (standard litre per minute) into a relatively small photolytic cell, such that the cell is replenished prior to each photolysis pulse. The lower flow rates (relative to the flow tube technique) through the cell minimise the consumption of ultra clean air for laboratory calibrations, and, since only a small central portion of the cell is photolysed by the laser, radical wall losses are minimised. A related remote sensing method, using a two laser pump-probe lidar, was proposed to measure the OH reactivity, but has not been used for routine measurements (Calpini et al., 1999).

In the recently developed Comparative Reactivity Method (CRM) (Sinha et al., 2008) the concentration of pyrrole (C_4H_5N), which is not normally present in the atmosphere, is measured by a proton transfer mass spectrometer as it titrates OH radicals that are artificially generated, either in the presence of an ambient air sample or with added zero air. When ambient air is present, OH sinks in the atmosphere remove some of the OH, and hence less pyrrole is removed, and a higher concentration of pyrrole is observed compared when just zero air is added. By recording the difference in (pyrrole) between when sampling ambient or zero air, the OH reactivity in the ambient sample can be determined.

The feedback from HO_2 to OH by reaction with [NO] (Reaction 5) may cause the OH reactivity, k' not to be faithfully represented by the measured relaxation time if the rate of feedback, which is dependent upon [NO], becomes significant compared with the rate of OH loss. A theoretical perturbation analysis for OH and HO_2 using a model system constrained by NO_x (Bell et al., 2003) concluded that a measurement of the OH relaxation time would indeed be representative of the atmospheric reactivity of OH radicals either at very low [NO] found in the clean boundary layer, or for highly polluted conditions when the rate of OH loss is high (e.g. by reaction with NO_2) compared with the rate of Reaction (5). We return to this point in more detail in Sect. 3.5 below. A key parameter is the HO_2/OH ratio that is initially generated in the OH reactivity field instrument. In the flow tube method, this ratio is at least 1 initially, and a correction to the observed k' must be made when ambient [NO]$>\sim$1 ppbv (Shirley et al., 2006). The pump-probe LIF method is influenced much less by ambient NO concentrations as initially (HO_2)=0. We return to the production of OH by recycling from HO_2 in Sect. 3.5.

In this work, the first method described above is employed to measure OH reactivity, namely measuring the decay of artificially produced OH in an atmospheric pressure flow tube reactor. OH radicals are generated in the tip of a movable injector tube which is co-axial with the much larger diameter main flow tube. The radicals mix into the ambient air flow through the main flow tube and react with trace gases. Downstream of the injector, gas from the main tube is sampled into a detection cell where OH radicals are detected by laser induced fluorescence. The decay of [OH] is measured as a series of individual OH signal measurement points by stepping the injector back in fixed increments to increase the distance from injection to sampling, thus increasing the time

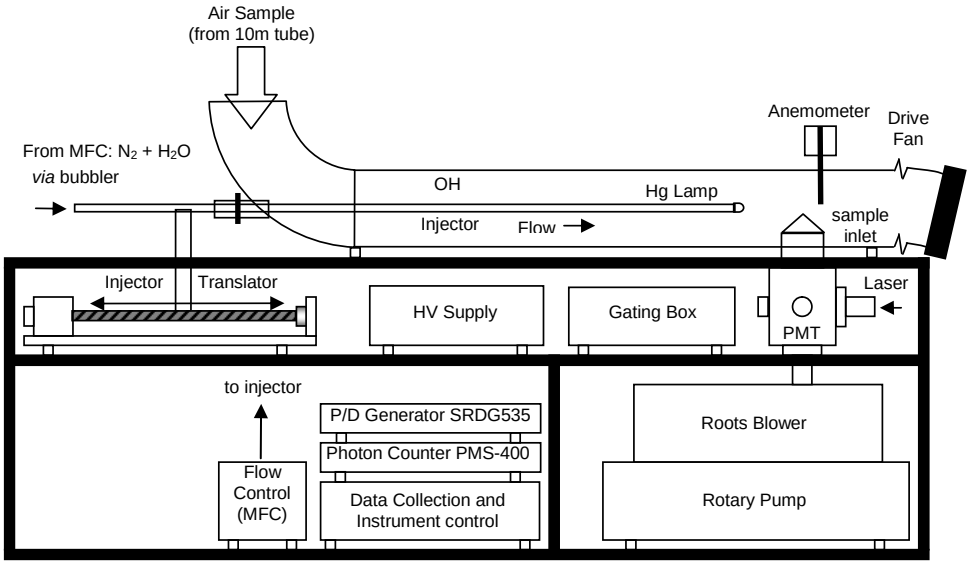

Fig. 1. Schematic diagram of the Leeds instrument to measure OH reactivity.

Table 1. Key operating parameters for the flow-tube OH reactivity instrument.

Sample Flow Rate	300–900 SLM
Flow Velocity	0.6–2.0 ms^{-1}
Reynolds Number	3950–13 200
Residence Time	2.5–0.75 s
Time Resolution	300 s
Limit of Detection	2 s^{-1}
Accuracy (<1, 1, 5, 10 ppbv [NO])	10, 10, 11, 13% (at 1 sigma)

available for OH to react with ambient trace gases. The flow velocity in the main flow tube is measured so that the distance, s, between the injector and the sampling point can be converted into a reaction time, t.

The [OH] generated in the flow tube is kept sufficiently low that pseudo-first-order conditions are maintained, thus the absolute OH concentration does not need to be known, although this can be obtained by calibration of the sensitivity of the LIF cell. OH undergoes exponential decay according to Eq. (3):

$$[OH]_t = [OH]_0 \exp\left(-(k' + k'_{wall})t\right) \quad (3)$$

where k' represents the reactive decay rate, the inverse of the chemical lifetime, τ_{OH}, given by:

$$k' = \Sigma k_i [X]_i \quad (4)$$

where $[X]_i$ represents the concentration of an atmospheric trace gas and k_i the rate coefficient for its reaction with OH at the temperature of the flow-tube, and k'_{wall} is the non-reactive loss of OH mainly due to wall losses. The main constituents reacting with OH are CO, CH_4, O_3, NO_2, NO, non-methane hydrocarbons, and oxygenated VOCs. The measured value of $k'+k'_{wall}$ is obtained by a least-squares linear regression fit to the plot of ln(OH signal) versus time, and after subtraction of k'_{wall} (obtained using zero-air) is compared to the calculated value of $\Sigma k_i [X]_i$ using co-measured sinks to identify the magnitude of unmeasured sinks.

2.1 Flow tube reactor

Figure 1 shows a schematic diagram of the instrument and Table 1 indicates the key operational parameters. Ambient air is pulled through a 6 m long, 10 cm ID Teflon lined sampling tube by a drive fan (Papst 4214) such that under typical operating conditions ca. 300 SLM is sampled with a residence time of ~10 s. The decay of OH is measured inside a 1.5 m long, 10 cm ID borosilicate glass flow tube. The air flow velocity at the centre of the flow tube is measured using a hot-wire anemometer (TSI Air Velocity Transducer 8455-150) and the rotational speed of the drive fan is adjusted to give an air velocity between 0.6 and 2.0 ms^{-1} (the velocity is adjusted depending upon ambient location so that it is possible to observe the OH decay through at least an order of magnitude of [OH] in clean and polluted areas). The flow tube operates at ambient pressure, and the gas temperature is measured via several thermocouples along the flow tube for use in subsequent kinetic analyses. The Reynold's Number (N_{Re}) is in the range 3950–13 200 for flow velocities 0.6–2 ms^{-1}. Under these flow conditions, and using N_{Re}=5000 as a criterion for turbulent flow, the flow is transitioning to turbulent to fully turbulent, which helps to mix rapidly the main gas flow with the output from the sliding injector.

OH (and HO_2) radicals are produced at the tip of the sliding injector, which is an aluminium tube (2 cm OD, ~1.6 cm ID) that is aligned coaxially with the flow tube, and which has a 6 cm long Teflon tip. A mass flow controller (Brooks Instruments, 5850S) is employed to meter ca. 5 SLM of N_2 (Air Products, 99.999%) first through a bubbler containing deionised water to humidify the gas, and then through the sliding injector. The photolysis of H_2O is performed at 185 nm using a Hg PenRay lamp (L.O.T.-Oriel 6035) which is housed inside the Teflon injector tip, which surrounds the lamp to shield it from the main gas flow and to minimise radical wall losses. OH radicals are produced directly inside the injector tip via H_2O photolysis (Reaction 10) but since N_2 is usually used as the carrier gas for the injector, the hydrogen atoms also produced either react with any O_2 impurity within the injector or almost instantaneously upon mixing into the main air flow, via Reaction (11). Experiments in which NO is added to the LIF FAGE (Fluorescence Assay by Gas Expansion) detection cell to convert HO_2 to OH (see below) show that HO_2 initially exiting the injector is in excess of OH by a factor of ca. 1.75, which is likely due to hydrogen atoms (or HO_2 formed by O_2 impurities) being less susceptible to wall loss on the Teflon injector tip than OH. Some experiments were conducted using zero air (Air Products 99.999%) as the injector gas, and gave identical measurements of k'. The rate constants for OH+O_3 and HO_2+O_3 are approximately 7×10^{-14} and 2×10^{-15} cm^3 $molecule^{-1}$ s^{-1}, respectively, (Sander et al., 2002) and ensure that at the levels of [O_3] generated in the injector when zero air is used, and following dilution into the main flow (typically <100 ppbv), there is no significant loss of OH or HO_2 via reaction with O_3.

To ensure thorough mixing, the injector gas flow is delivered into the main gas flow through a series of 20 holes (1.0 mm diameter) drilled radially into the tip and 5 mm from its end so that the gas is forced out orthogonally to the main flow tube central axis. The injector generates ca. 10^{10} molecule cm^{-3} OH and HO_2, which are diluted by a factor of 60 when mixed into the main flow, and typically an OH decay is measured from an initial [OH] of ca. 10^8 molecule cm^{-3}, the absolute concentration being obtained via calibration of the sensitivity of the FAGE LIF cell (see Sect. 3.1 below). This concentration of OH provides a very good signal-to-noise ratio, and is sufficiently low so self- or cross-reactions of OH and HO_2 can be neglected once the injector gas has mixed into the main flow, and ensures that pseudo first-order conditions, [OH]$\ll$[X] are maintained, i.e. the OH co-reactant concentrations are not depleted to any significant extent during a decay. The 10 s residence time in the sampling tube completely removes any influence from ambient OH, and although the lifetime of ambient HO_2 under clean conditions is significantly longer than 10 s, no HO_2 signal is observed with the Hg pen-ray lamp switched off.

The position of the sliding injector is controlled by a linear drive (BSL Engineering KR4610A) to better than 0.25 mm (corresponding to 0.25 ms uncertainty in the reaction time for 1 ms^{-1} flow velocity) and the reaction time of OH with trace gases in the sampled air is determined by knowing the injector position and a measurement of the flow velocity by the anemometer. The injector start position is typically s=11.5 cm upstream of the fluorescence cell sampling point, which ensures that the gas from the injector is well mixed into the main gas flow prior to sampling (see Sect. 3.2 below). Measurements are typically made by stepping the injector back progressively until its tip is s=29.5 cm upstream of its start position. The injector is coupled to the flow tube via a neoprene sealing gasket which prevents any external air entering the flow tube at this interface, as confirmed by overfilling the external area around the seal with an injection of butane and observing no loss of OH signal.

2.2 Laser induced fluorescence (LIF) cell

Downstream of the injector, air is sampled from 1.5 cm below the central axis of the main tube into a FAGE (Fluorescence Assay by Gas Expansion) detection cell where OH is detected by LIF near 308 nm using the $Q_1(1)$ transition of the $A^2\Sigma^+$ (v'=0)-$X^2\Pi_{3/2}$ (v''=0) band. The cell is constructed from aluminium and all surfaces are black-anodised to minimise the scattering of laser radiation. The main cell body consists of a ca. 150 mm cube which has been machined to provide three orthogonal axes. The cell is maintained at a pressure of ca. 1 Torr (measured using MKS 722 Baratron) by a roots/rotary pump combination (Leybold Vacuum D65B/WUA500) which draws a flow of ca. 4 SLM of air vertically downwards through a 0.8 mm diameter pinhole, creating a supersonic expansion. The main vertical bore through the cell is 100 mm internal diameter. The cell has a port to allow the addition of 1–2 sccm of nitric oxide [NO] downstream of the supersonic expansion so that [HO_2] can be measured after it has been converted to OH via Reaction (5).

Pulsed laser-light (5 kHz pulse repetition frequency) is delivered via an optical fibre (Oz Optics, QMMJ-55-UVVIS, fibre transmission ca. 60%) and at the cell the fibre is connected to collimating optics (Oz Optics, HPUCO-25-308-M-25PQ) at the end of a baffled side-arm orthogonal to the gas flow. The light enters the cell ca. 120 mm below the sampling pinhole. The light passes through the cell and out of another baffled side-arm to a photodiode (New Focus Large Area Photoreceiver 2032) to measure the average laser power to permit subsequent normalisation of the LIF signal for fluctuations in laser power. Fluorescence from OH radicals excited by the laser pulse is collected on the third orthogonal axis and is filtered (308 nm bandpass filter, FWHM 1 nm, transmission >0.50 at 308 nm, transmission $<10^{-6}$ at other wavelengths, Barr Associates) before being focussed onto the photocathode of a channel type photomultiplier tube

(PMT) (Perkin Elmer, C-943P operated at −3 kV) specifically designed for photon counting. Since an on-resonance LIF scheme is used to detect OH, the PMT is gated off during the laser pulse (35 ns FWHM pulse duration) to prevent saturation and after-pulsing, and gated back on ca. 100 ns after the laser pulse to collect fluorescence photons (typically for 1 μs). After a 10 μs delay, a background signal is then collected (typically for 10 μs), which arises from any solar radiation which may enter the cell through the sampling pinhole and PMT dark counts (ca. 1 count per second). The solar background at 308 nm is removed totally by the glass flow tube. The fluorescence signal is then corrected for the laser background by subtraction. Discrete photon signals from the PMT are processed using a multi-channel scaler card (Becker and Hickl, PMS 400, minimum bin width 250 ns). The timing of the measurement is controlled by a delay generator (SRS DG535), which triggers the laser, the photon counter, and supplies a TTL gate signal to the PMT gating box.

2.3 Laser system

The laser employed is a tuneable, high pulse-repetition-frequency, solid state Nd:YAG pumped titanium sapphire laser, and has been described in detail elsewhere (Bloss et al., 2003). Briefly, the pump laser beam is provided by a diode-pumped, Q-switched, intra-cavity frequency doubled Nd:YAG laser (Photonics Industries DS 20-532), capable of producing ca. 12 W of 532 nm radiation when operated at a pulse repetition frequency of 5 kHz, with a typical pulse length of 25 ns. The Nd:YAG second harmonic at 532 nm is used to pump the Ti:Sapphire laser, producing broadband near-IR radiation in the range 690–1000 nm (Photonics Industries TU-UV 308). The desired Ti:Sapphire oscillator wavelength is selected using a diffraction grating whose incident angle is computer controlled. The Ti:Sapphire oscillator is operated at 924 nm. The 924 nm radiation is frequency tripled via two non-linear stages, using the first CLBO (cerium lithium borate) crystal to generate the second harmonic at 462 nm, and the second CLBO crystal to perform sum-frequency mixing of this wavelength with the fundamental (924 nm) to obtain the desired 308 nm radiation. The system is capable of producing up to 150 mW of UV radiation at 308 nm, when operated at a pulse repetition frequency of 5 kHz, equivalent to 30 μJ per pulse. The UV beam is approximately 3 mm in diameter, with a typical pulse length of 35 ns, and a spectral bandwidth of 0.065 cm^{-1}. The laser bandwidth is well matched with the lineshape of a single OH rotational transition at ca. 308 nm (OH $A^2\Sigma^+ \leftarrow X^2\Pi_i$ (0,0) transition) that has a Doppler-broadened profile of ca. 0.08 cm^{-1} under FAGE measurement conditions. The UV output of the laser is coupled into the optical fibre via micrometer positioned coupling mounts (Elliot Scientific MDE511-SPEC), and 5–10 mW of laser power is finally delivered to the FAGE cell.

2.4 Reference cell

A constant, small fraction of the laser power (ca. 1 mW) at 308 nm is passed through a small reference fluorescence cell in which a relatively high, stable concentration of OH is produced by microwave discharge or heated filament induced dissociation of water vapour in humidified air at a pressure of ca. 2 Torr. The fluorescence is collected in a similar manner as that described above for the FAGE cell, and processed by the photon counting technique. The signal from this cell provides a laser wavelength calibration, and is used to determine the centre of the particular OH transition required for on-line measurements, and also to tune the laser to a closely adjacent wavelength off the OH transition where there is no absorption by OH, for off-line background measurements.

2.5 Instrument control

The controlling computer is programmed to automatically manage the measurements, archive all measurement data and housekeeping information, and perform preliminary analysis of the OH decays to yield the decay rate and extrapolated OH signal at zero injector distance (and their respective 1-sigma statistical uncertainties). The delay generator is controlled with a GPIB interface, whereas analogue signals from the anemometer, flow controller, pressure head, and laser power photodiode are digitised by an A/D card (Measurement Computing, PCI-DAS 1200), and the linear drive and the laser are controlled via RS232 interfaces. The instrument is housed in a 19 inch rack system, and all electrical power is supplied via an uninterruptible power supply (APC 1000VA).

2.6 Measurement of OH decay rates

To measure OH decay rates, the data acquisition cycle begins by scanning the laser to find the centre wavelength of the OH $Q_1(1)$ rotational line at ∼308 nm using the reference cell. The laser is then held at this wavelength typically for two decay measurements, and then the laser is stepped off the OH transition to measure the signal due solely from scattered laser light; this smaller, off-line signal is subsequently subtracted from each of the signals collected during the OH decay measurement.

With the laser wavelength tuned on-line, an OH decay measurement commences with the injector in its start position ca. s=11.5 cm upstream of the FAGE cell sampling pinhole. OH fluorescence signal, average velocity, average laser power, cell pressure, injector flow rate, main flow gas temperatures, and PMT voltage and current are acquired every second during an integration period of typically 30 s, and then the injector is pulled back by a fixed step length typically 20 mm. This process is repeated until 10 data points on a decay are acquired, then the injector is returned to its start position and the process is repeated so that two decays are measured. As described above, the laser wavelength is

then tuned off-line to measure the signal from laser scatter every second for the same integration period (i.e. 30 s) as the on-line measurements. The signals are then normalised point-by-point for any changes in laser power that took place during the decay. This overall process is repeated automatically such that ca. 10 OH decays are recorded every hour. The OH reactivity instrument shares the same laser as is used for measurements of ambient OH and HO_2 radicals using FAGE, and the data acquisition cycle for the OH reactivity measurements (for example the number of points in each decay) has been designed to match in with the duration of the wavelength on- and off-line periods for the [OH] and [HO_2] measurements.

Figure 2 (lower two decays) shows examples of field measurements of OH decays under low [NO] (<1 ppbv) conditions such that there is insignificant recycling of HO_2 to OH. The random statistical error in the fitted values of $k'+k'_{wall}$ shown is ~1–2%, and is mostly dependent upon laser stability and the (unknown) temporal variability of the OH sinks. An additional error of $\pm 0.4\,s^{-1}$ on the value of k' takes into account the error in k'_{wall} which has to be subtracted. There is a systematic error of 10% in the measurement of the reaction time, which arises from the calibration of the flow velocity measured by the anemometer, whose accuracy is controlled by the uncertainty of rate constants for the removal of OH by known amounts of added sinks (see Sect. 3.3 below). The accuracy is reduced slightly in the presence of enhanced levels of NO as a recycling correction has to be applied (see Sect. 3.5 below).

For characterisation experiments, N_2 bath gas was delivered via a 0–1000 SLM variable-area flow meter (Omega Engineering, Inc., FL-1504A) into a 19 L reservoir, and the sampling line drew the gas from this reservoir. This arrangement allowed the use of flow conditions in the flow tube very similar to those during ambient atmospheric sampling. Gaseous reactant mixtures were added via mass flow controllers (MKS Instruments, 1179A) through a T-piece attached to the top of the variable-area flow meter.

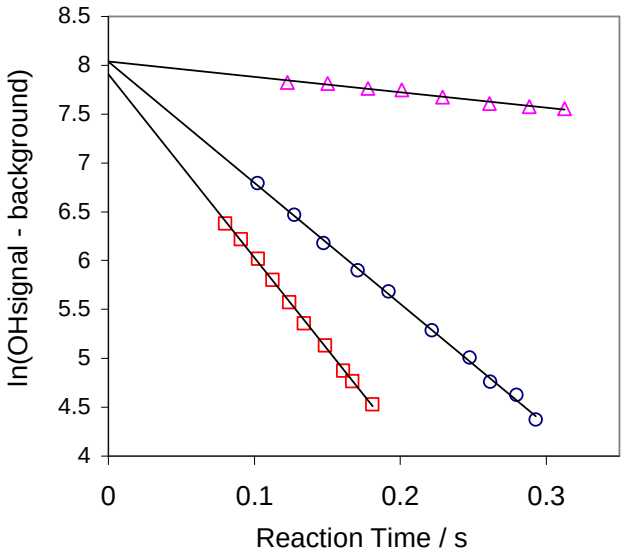

Fig. 2. Pseudo-first-order decays of ln (OH signal – background) versus reaction time. The upper decay (Δ) was obtained using zero-air in the laboratory, and the solid line is a linear-least squares fit to these data, the gradient of which gives a wall loss rate of $1.88\pm0.09\,s^{-1}$. The two lower decays (◯ and □) are examples from field measurements, the solid lines are fits to these data which give OH reactivities of $12.46\pm0.15\,s^{-1}$ and $18.59\pm0.21\,s^{-1}$, respectively, after correction for the wall loss. The errors quoted are the 1 sigma random errors from the linear least-squares fitting routine.

3 Results and discussion

3.1 FAGE cell calibration

While the absolute [OH] is not required for the measurement of the OH reactivity, knowledge of [OH] and [HO_2] are essential in correcting for the effect of any HO_2 to OH feedback. The sensitivity of the FAGE cell was calibrated using an OH (and HO_2) source in which the OH (=HO_2) concentration can be produced in concentrations between 10^7 and 10^{10} molecule cm^{-3}. The OH and HO_2 radicals are produced by the 185 nm photolysis of a known concentration of H_2O vapour in humidified ultra-clean air via reactions (Eq. 5) and (Eq. 6). The calibration system uses an O_2 chemical actinometer to determine the product of the flux of 185 nm radiation and photolysis time which is required to calculate [OH] (Schultz et al., 1995; Bloss et al., 2003; Heard and Pilling, 2003).

The calibration yielded a cell sensitivity for OH of $\sim 5\times10^{-8}$ cts s^{-1} molecule^{-1} cm^3 mW^{-1}, which results in a detection limit of $\sim 5\times10^6$ molecule cm^{-3} for typical laser powers of a few mW, background counts of $3\,s^{-1}$, a signal-to-noise ratio of 1, and for 30 s integration time. This cell sensitivity and limit of detection was adequate to measure OH decays from initial concentrations which were in the region of 10^8 molecule cm^{-3}.

3.2 Determination of flow characteristics

The OH radicals generated inside the tip of the sliding injector must be fully mixed into the main ambient flow on a short timescale relative to the OH lifetime. In order to probe the mixing of the injector gas flow into the main air flow the injector humidified N_2 flow was replaced with a flow of zero air in order to generate a stable concentration of O_3 inside the injector via the 185 nm photolysis of O_2 followed by Reaction (7). A commercial analyser (Thermo Electron 49, detection limit 0.5 ppbv) was used to measure both the axial and the radial [O_3] profiles downstream of the injector by inserting the analyser's sampling tube (6 mm OD) into the

main flow tube through a series of ports along the tube. To obtain a radial profile, $[O_3]$ was measured at 10 points orthogonal to the flow direction, whereas an axial profile was obtained by measuring $[O_3]$ on the flow tube cylindrical axis at 10 points downstream of the injector.

With typical injector flows (5 SLM) and main tube flows (300 SLM), uniform axial and radial $[O_3]$ profiles with no gradients were observed for distances greater than 10 cm from the injector, indicating that the injector gas was completely mixed into the main flow after this point. Rapid mixing is expected for the turbulent regime within the flow tube. No evidence for losses of O_3 at the walls was observed. Typically, the injector was placed ca. 11.5 cm upstream of the FAGE cell sampling point at the beginning of the measurement, and the observed decay of OH signal for $s>11.5$ cm was always described by a single exponential function. For $s<11.5$ cm significant deviation from single exponential decay behaviour was observed in the first few points on the decay; the initial rate of decay was around a factor of 2 higher due to incomplete mixing/dilution compared to the rate of decay when fully mixed. Additionally, by varying the air velocity in the flow tube from ca. 0.6 to 2.0 m s^{-1} it was demonstrated that the measured decay rate k' was independent of flow velocity.

3.3 Calibration of the flow velocity

In order to determine the reaction time, t, of OH radicals with trace gases a hot-wire anemometer was used to measure the average flow velocity, v, in the main tube, using $t=s/v$. The calibration of the anemometer was performed by adding a known flow of a single trace gas, X, which reacts with OH to an ultra-clean (Air Products 99.999%) main flow of air, and measuring the pseudo-first order rate of decay of OH, r, which is given by:

$$r = k' + k'_{\text{wall}} = k_{\text{OH+X}}[\text{X}] + k'_{\text{wall}} \quad (5)$$

where [X] is the concentration of the added trace gas. The value of r is determined as a function of [X], and a second-order plot of r against [X] yields a gradient equal to $k_{\text{OH+X}}$ and intercept k'_{wall}, being a sum of wall losses and reactions of OH with impurities in the main flow of zero air. Comparison of the measured $k_{\text{OH+X}}$ with the recommended literature value enables the accuracy of the reaction time, t, and hence flow velocity, v, to be evaluated.

The above procedure was performed for X=CO and n-hexane, for which $k_{\text{OH+CO}}=(2.41\pm0.18)\times10^{-13}$ and $k_{\text{OH+hexane}}=(5.51\pm0.47)\times10^{-12}$ cm^3 molecule^{-1} s^{-1} were obtained, the errors representing 1σ sigma random error from the gradient of r against [X]. The results are in excellent agreement with the JPL recommendation (Sander et al., 2002) of $k_{\text{OH+CO}}=(2.41\pm0.72)\times10^{-13}$ cm^3 molecule^{-1} s^{-1} and in good agreement with the literature value of $k_{\text{OH+hexane}}$ $(5.20\pm1.04)\times10^{-12}$ cm^{-3} s^{-1} (Atkinson, 2003). For a range of trace gases the agreement between measured and recommended literature values of rate constants was found to be very good. No additional calibration of the anemometer was undertaken. We therefore place a 10% (1σ) error on the accuracy of v, and hence t, reflecting the uncertainty in the rate constant for the removal of OH by the added trace gas. It should be noted that this experimental arrangement potentially offers an accurate method to determine rate constants at atmospheric pressure, as the concentration of the free-radicals is extremely low, and the loss of OH via secondary reactions, for example with products of the initial reaction, is negligible.

3.4 Determination of the rate of the wall loss

For ambient sampling, the value of k'_{wall} should mainly be determined by wall loss as opposed to dilution of the injector flow since OH decays were always measured after the injector flow was well mixed into the main flow, as determined by the O_3 profile measurements described above. In the laboratory, however, k'_{wall} will also have a contribution from impurities in the main flow of gas, which are difficult to completely remove. A range of high purity air and nitrogen (Air Products 99.999% and BOC 99.999%) from several batches were employed, as well as boil-off from a liquid nitrogen Dewar, to supply the main tube flow and N_2 for the injector flow. For some gas batches, hydrocarbon impurities were quantified using gas chromatography and NO_x using a commercial trace gas analyser (Thermo Electron 42 TL, detection limit 50 pptv). For most gases used, no significant levels of C_2–C_8 hydrocarbons were observed (detection limit 5–10 pptv), but significant levels of NO_x were sometimes observed, for example ppbv levels of NO_2, which are difficult to completely scrub from a 300 SLM flow, and will give some contribution towards k'_{wall}. The measured wall loss rate from a series of measurements was determined to be 1.6 ± 0.4 s^{-1}, after taking into account measured impurities, where the error represents 1 standard deviation of all measurements. An example of a laboratory measurement of the wall loss rate is shown in the upper trace of Fig. 2.

Measurements of the decay of HO_2 radicals, with NO added to the FAGE cell to convert HO_2 to OH (which is then excited by LIF) gave a physical loss rate of ~1 s^{-1}. The concentration of NO impurity in the main flow cannot account for this loss. This value is not significantly less than observed for OH, and since HO_2 is expected to have a lower wall loss rate than for OH, implies some of the physical loss for HO_2, and therefore OH, maybe due to axial dilution in the flow (e.g. residual radial mixing or diffusion) away from the injector. It is not crucial to understand the mechanism of the physical loss, rather that a determination of k'_{wall} is made under the same sampling conditions used in the field. Kovacs et al. (2003) also used the flow LIF method and reported a larger OH wall loss rate of 5 s^{-1} in a similar diameter glass flow tube, and for a recently developed aircraft version of

this instrument, an OH wall loss of $2.9\,s^{-1}$ was reported, although $\sim 1\,s^{-1}$ of this was ascribed to the presence of trace impurities in the carrier gases used (Mao et al., 2009). The difference in the physical loss rate between these flow-tube based instruments is the result of the differences in the flow profiles or nature of the walls. In the present work, the flow regime was selected which gave a compromise between the time taken to mix the injector gas into the main flow gas and the OH signal stability after mixing such that the measured decays were described by a single exponential. Laminar flow conditions were attempted but the reduced flow velocity required (for the same diameter flow tube) resulted in excessive mixing times such that a significant fraction of OH was removed prior to pulling back the injector to measure a decay. In the present work, and that of Kovacs et al. (2003) under laminar flow conditions, k_{wall} is an empirical, reproducible quantity.

3.5 Quantifying OH feedback from the reaction HO_2+NO→OH+NO_2

A major disadvantage of the flow tube method is the production of hydrogen atoms in the injector (Reaction 10), as these react rapidly with any O_2 impurity in the injector N_2 flow and O_2 in the ambient air flow to form HO_2 radicals (Reaction 11). Any recycling reaction that converts HO_2 to OH could potentially lead to an observed decay of OH that is not representative of the true OH reactivity, k'. At typical tropospheric concentrations of O_3, the reaction HO_2+O_3 does not constitute any significant recycling to OH. However, if significant NO is present in ambient air, the reaction of HO_2 with NO may generate enough in situ OH to perturb the measured decay.

Bell et al. (2003) have characterised this process theoretically using a perturbation analysis to investigate the relationship between the inverse of the true atmospheric lifetime $(\tau_{OH})^{-1}=k'$, due to reaction of OH with all of its sinks, and the decay time (or eigenvalues, $-\lambda$). In a model study, a perturbation was applied to [$O(^1D)$], with subsequent increases in [OH] and [HO_2], for [NO_2]/[NO]=0.1 and 5 over a broad range of [NO]. The eigenvalues and chemical lifetimes for OH and HO_2 were calculated using Jacobian methods and the extent of coupling between OH and HO_2 investigated (Bell et al., 2003). The feedback from HO_2 to OH can lead to a non-equivalence of $(\tau_{OH})^{-1}$ and $-\lambda$, depending on the size of the feedback term and the difference in the atmospheric lifetimes of OH (τ_{OH}) and HO_2 (τ_{HO2}). For this model, at low [NO] (<1 ppbv), typical of background tropospheric conditions, it was found that for the two [NO_2]/[NO] ratios studied (0.1 and 5), there is a significant time-scale separation between the lifetimes of OH and HO_2, $(\tau_{OH})^{-1}>>(\tau_{HO2})^{-1}$, and feedback via HO_2+NO does not cause a significant deviation between $-\lambda$ and τ_{OH}^{-1}. At higher [NO] the behaviour depends upon [NO_2]/[NO], but for an atmospherically realistic ratio of 5, τ_{OH}^{-1} is always

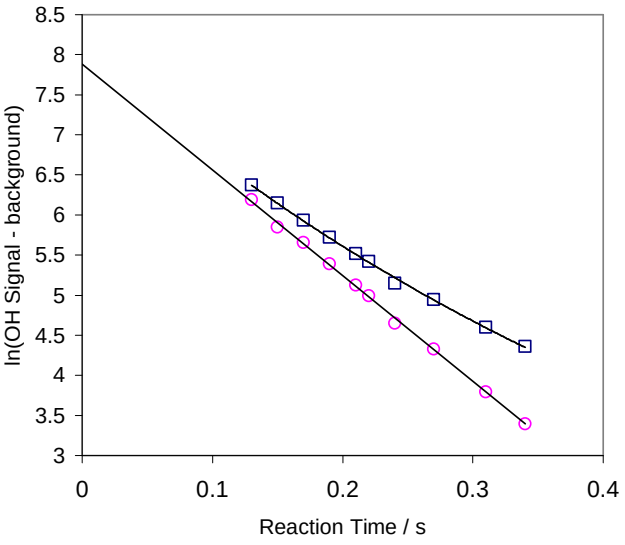

Fig. 3. An example of the influence of OH formation from the reaction HO_2+NO→OH+NO_2 on a decay of OH measured in the field. The upper trace (□) shows a slight upward curvature in the observed OH decay for [NO]=3.74 ppbv, and the lower trace (◯) shows the result of the correction (using Eq. (7) giving a good linear relationship between ln (OH Signal) and reaction time, yielding the true decay rate of $13.20\pm0.30\,s^{-1}$. The error quoted is the 1σ random error from the linear least-squares fitting routine.

greater than τ_{HO2}^{-1} under all conditions of [NO], and except at some intermediate [NO], the decay rate $-\lambda$ tracks the reciprocal lifetime τ_{OH}^{-1} closely. The lifetime ordering in the troposphere is assured as k_{OH+NO_2} is larger than k_{HO_2+NO} and under steady-state conditions [NO_2]>[NO]. In addition, the concentrations of VOCs are expected to increase simultaneously with NO_x thereby further decreasing the OH lifetime relative to that of HO_2. Bell et al. (2003) also modelled a field experiment under mostly clean conditions in the marine boundary layer, and showed that the decay rate $-\lambda$ tracks the reciprocal lifetime τ_{OH}^{-1} closely except for some periods of elevated [NO] during pollution episodes.

A conclusion of the perturbation study was that except under clean conditions checks should be made for any non-equivalence between τ_{OH}^{-1} and $-\lambda$. In the current experiment, the effect of HO_2 recycling on the OH decay may be larger than the Bell et al. (2003) study as immediately after the injector the ratio [HO_2]/[OH] may be greater than unity due to smaller surface losses of HO_2 following production in the injector. Indeed, as shown in the upper trace of Fig. 3, there is a deviation from single exponential behaviour (a slight positive curvature) of OH towards the end of a decay measured for [NO]=3.74 ppbv. [NO] in the ambient air was measured using a commercial NO_x analyser (Thermo Electron 42 TL, detection limit 50 pptv). However, given knowledge of absolute [OH] and [HO_2] along the flow, together with a measurement of [NO], it is possible to correct for any recycling

by NO using a numerical integration method (Shirley et al., 2006; Kovacs et al., 2003). If HO_2+NO is the only source of OH, then:

$$\frac{d[\mathrm{OH}]}{\mathrm{dt}} = -(k' + k'_{\mathrm{wall}})[\mathrm{OH}] + k_{\mathrm{HO_2+NO}}[\mathrm{HO_2}][\mathrm{NO}] \quad (6)$$

$$= -(k' + k'_{\mathrm{wall}})[\mathrm{OH}] + k_{\mathrm{HO_2+NO}} R [\mathrm{OH}][\mathrm{NO}] \quad (7)$$

where $R = \frac{[\mathrm{HO_2}]}{[\mathrm{OH}]} = \frac{S_{\mathrm{HO_2}}}{S_{\mathrm{OH}}} \frac{C_{\mathrm{OH}}}{C_{\mathrm{HO_2}}}$, and S_{X} and C_{X} are the observed LIF signals and experimentally calibration factors, respectively, for OH and HO_2. If R is assumed constant from the beginning to the end of each injector step in the measured OH decay (change in reaction time Δt), then integration of equation (Eq. 7) gives:

$$[\mathrm{OH}]_{\Delta t} = [\mathrm{OH}]_0 \exp(-(k' + k'_{\mathrm{wall}})(\Delta t)) \exp(k_{\mathrm{HO_2+NO}}[\mathrm{NO}] R (\Delta t)) \quad (8)$$

where $[\mathrm{OH}]_0$ and $[\mathrm{OH}]_{\Delta t}$ are the OH concentrations at the initial and subsequent position of the injector during the decay, respectively. Taking logs and rearranging gives (Kovacs et al., 2003):

$$k' + k'_{\mathrm{wall}} = -\frac{\Delta \ln[\mathrm{OH}]}{\Delta t} + k_{\mathrm{HO_2+NO}}[\mathrm{NO}] R = -\frac{\Delta \ln S_{\mathrm{OH}}}{\Delta t} + k_{\mathrm{HO_2+NO}}[\mathrm{NO}] \frac{S_{\mathrm{HO_2}}}{S_{\mathrm{OH}}} \frac{C_{\mathrm{OH}}}{C_{\mathrm{HO_2}}} \quad (9)$$

where Δ ln [OH]=ln $[\mathrm{OH}]_0$-ln$[\mathrm{OH}]_{\Delta t}$. Hence knowledge of the LIF signals S and calibration factors C for both OH and HO_2 enables a correction to be made to the value of $k' + k'_{\mathrm{wall}}$ for a time period Δt, the reaction time between adjacent points in the decay. To utilise the entire decay to correct the value of $k' + k'_{\mathrm{wall}}$, a similar procedure must be repeated for each point in the decay (Shirley et al., 2006). For the first two points in the decay, $\Delta t = t_1 - t_0$, and integration of Eq. (7) gives:

$$[\mathrm{OH}]_1 = [\mathrm{OH}]_0 \exp(-(k' + k'_{\mathrm{wall}})(t_1 - t_0)) \exp(k_{\mathrm{HO_2+NO}}[\mathrm{NO}] R (t_1 - t_0)) \quad (10)$$

where $[\mathrm{OH}]_0$ and $[\mathrm{OH}]_1$ are the OH concentrations at position 0 ($t = t_0$) and position 1 ($t = t_1$) of the injector during the decay. Without the recycling from HO_2 the true OH concentration at $t = t_1$ is given by:

$$[\mathrm{OH}]_{\mathrm{true}_1} = [\mathrm{OH}]_0 \exp(-(k' + k'_{\mathrm{wall}})(t_1 - t_0)) \quad (11)$$

and hence the value of $[\mathrm{OH}]_1$ at position one can be corrected (Shirley et al., 2006) to give:

$$[\mathrm{OH}]_1^c = [\mathrm{OH}]_1 \exp(-k_{\mathrm{HO_2+NO}}[\mathrm{NO}] R (t_1 - t_0)) = [\mathrm{OH}]_1 (\exp - k_{\mathrm{HO_2+NO}}[\mathrm{NO}] \frac{[\mathrm{HO_2}]_{\mathrm{average}}}{[\mathrm{OH}]_{\mathrm{average}}} (t_1 - t_0)) \quad (12)$$

where $[\mathrm{HO_2}]_{\mathrm{average}}$ and $[\mathrm{OH}]_{\mathrm{average}}$ are the average of the concentrations at injector position 0 and 1. As the OH and HO_2 concentrations are related to the observed signal by the measured calibration factors, the correction can be made. The procedure is then repeated to further correct the signal at position 2, which is at a longer time t_2, and so on to the end of the decay. Figure 3 (lower trace) shows the result of such a correction applied to the OH decay for a high concentration of [NO]=3.74 ppbv, using the measured $[\mathrm{HO_2}]/[\mathrm{OH}]$ ratio as a function of injector position. The corrected decay rate is $13.20 \pm 0.30\,\mathrm{s}^{-1}$ (1σ) compared to $\sim 9.5\,\mathrm{s}^{1}$ obtained from a linear-least-squares fit to the curved upper trace. For many applications, [NO] is considerably less than this, and the required correction is much smaller, but knowledge of [NO] and the ratio $[\mathrm{HO_2}]/[\mathrm{OH}]$ makes the correction straightforward to apply, but increases the uncertainty in the measured reactivity. The overall uncertainty associated with the NO correction comes from the uncertainty in the measured [NO] (5%), the uncertainty in the $[\mathrm{HO_2}]/[\mathrm{OH}]$ ratio (1.75 ± 0.2), and the uncertainty in the rate constant for reaction R5 (15%) (Sander et al., 2002). These uncertainties propagate in a linear fashion, but the overall uncertainty does increase with increasing [NO]. The increased uncertainties for 1, 5, and 10 ppbv of NO are 1.2%, 4.9%, and 8.1%, respectively.

Shirley et al.(2006) validated this correction procedure in the laboratory for [NO] in the range 10–200 ppbv, and after correction of the decays using the above method, found good agreement (within 15%) between the corrected reactivity and that calculated from [NO], using various amounts of added CO (together with impurities in the zero air) to react with OH. It is not necessary in the field to continuously determine $[\mathrm{HO_2}]/[\mathrm{OH}]$ with injector position (from subsequent OH and HO_2 decays) for every OH decay, rather to determine the $[\mathrm{HO_2}]$ decay occasionally, and use the continually measured [NO] to apply the correction.

Extrapolating the measured $[\mathrm{HO_2}]/[\mathrm{OH}]$ in the measured decay back to $t = 0$ at the injector tip gave $[\mathrm{HO_2}]/[\mathrm{OH}] = 1.75 \pm 0.2$, the error representing 1σ of all measurements, consistent with the $[\mathrm{HO_2}]/[\mathrm{OH}]$ ratio measured immediately after the gas exits the injector tip. This ratio is also consistent with a value of 3 reported by Kovacs et al. (2003) who employed a similar Teflon injector tip. Clearly, for a higher value of $[\mathrm{HO_2}]/[\mathrm{OH}]$, there is a larger influence from recycling, and the pump-probe OH reactivity instruments, as described in Sect. 2 above, for which, at least initially, $[\mathrm{HO_2}]=0$, have a significant advantage in polluted regions.

As a further test of the validity of the correction procedure outlined above for OH recycling from HO_2+NO, a full model of the chemistry within the flow tube was constructed using the *Master Chemical Mechanism* (MCM v 3.1) (Saunders et al., 2003; Jenkin et al., 2003, also see http://mcm.leeds.ac.uk/MCM/) and solved using Facsimile (Curtis and Sweetenham, 1987). The model was initialised with measured values of [OH] and $[\mathrm{HO_2}]$ exiting the flow-tube injector (after mixing), over a range of [NO], and using typical concentrations of CH_4, CO, NO_2, non-methane hydrocarbons and oxygenated

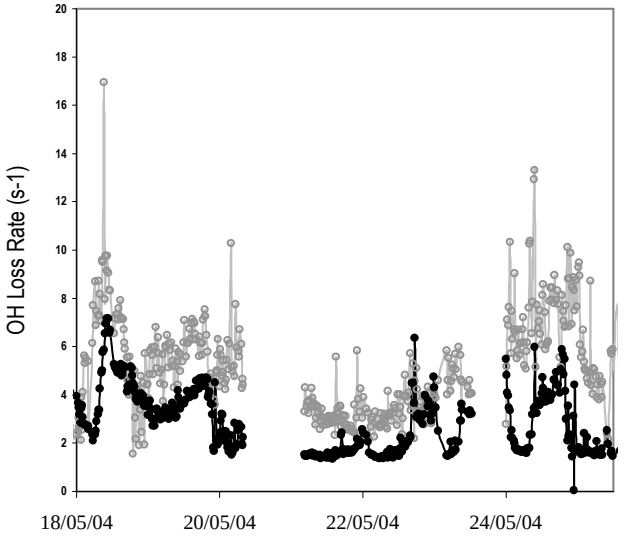

Fig. 4. A selection of a time series of OH reactivity measured during the TORCH-2 field campaign held at the Weybourne Atmospheric Observatory, Norfolk, UK, in May 2004. The grey points and grey line show the measured OH reactivity (error bars are not shown for clarity, typical error of 10% at 1 sigma), where the filled black points and black line show the OH reactivity calculated from the supporting measurements of OH co-reactants.

VOCs measured during the TORCH (Tropospheric Organic Chemistry Experiment) 2 field campaign held at the Weybourne Atmospheric Observatory (WAO), which took place in April–May 2004 (further details are given in Sect. 4.2 below). Time profiles of OH were calculated for an equivalent reaction time during the measurement of an OH decay, with and without the feedback step that recycles OH from HO_2+NO. The magnitude of the change to the value of k' due to recycling was very similar to the simple treatment using equation (Eq. 7), and the simple treatment was employed to correct field time-series due to its ease and speed of use.

4 Field measurements of OH reactivity

In this section a flavour of the field measurements made with the instrument are briefly presented, focussing only on the performance of the instrument and corrections made to account for OH recycling from HO_2+NO. Further analysis of the data and comparison with modelling calculations will be presented in future publications.

4.1 TORCH-2, Weybourne Atmospheric Observatory, Norfolk, April–May 2004

The reactivity instrument was deployed during the TORCH-2 campaign held at the Weybourne Atmospheric Observatory (52.57° N, 1.70° E), on the north Norfolk coast, in April–May 2004. The air sampled at Weybourne is generally a combination of aged air masses following chemical processing of gas and aerosol species during transport within the boundary layer, and cleaner marine air due to its coastal position. However, during TORCH-2, air masses of marine origin dominated with generally low [NO] and low OH reactivity. Although the $[HO_2]/[OH]$ ratio in the flow-tube was characterised, enabling accurate corrections to be made, these were relatively minor on account of the low [NO] (<1 ppbv). There was a detailed set of measurements of OH sinks (Lee et al., 2009).

Figure 4 shows a comparison between measured and calculated OH reactivity for the period 18th–25th May 2004. For almost all of this period the measured OH reactivity is greater than that calculated from measurements of OH co-reactant concentrations (e.g. NO_x, CO, methane, non-methane hydrocarbons, oxygenated hydrocarbons), and the general temporal trends in the measured and calculated loss rates are very similar which confirms that the instrument responds well to changing atmospheric composition. There are several rapid increases in the measured reactivity which are not captured in the calculated data. This may be due to the fact that the loss rate measurements are made at a greater frequency (2 min) than the co-reactant measurements (20 min), and the occurrence of these spikes correlates very strongly with plumes from observed shipping coming from the North Sea. A full interpretation of these data will be presented in a forthcoming publication (Lee et al., 2009), but it can be concluded from these data that the full range of OH co-reactants has not been fully characterised in the TORCH-2 campaign.

4.2 OP-3, Bukit Atur, Danum Valley, Sabah, Borneo, Malaysia, April–May 2008

The most recent OH reactivity measurements were made as part of the Oxidant and Particle Photochemical Processes above a SE Asian Tropical Rainforest (OP3) project, the first phase of which took place in April–May 2008. The objectives of the project were to understand how emissions of reactive trace gases from a tropical rain forest mediate the regional scale production and processing of oxidants and particles in the troposphere, and to better understand the impact of these processes on local, regional and global scale atmospheric composition, chemistry and climate. The reactivity instrument was located at the Bukit Atur Global Atmospheric Watch station, Danum Valley, Malaysia, Borneo (5.0° N, 117.8° E) and operated from within the University of Leeds FAGE shipping container. The inlet was located on the roof of the container, approximately 5 m above the ground, and measurements of OH, HO_2, NMHC, o-VOCs, CO, O_3, NO and NO_2 were all co-located close to the inlet. With the shipping container located in a forest clearing on a ridge, the sampling point was approximately 20 m below the forest canopy.

The Bukit Atur location was characterised by low NO_x (NO typically less than 100 pptv) and low ozone (typically

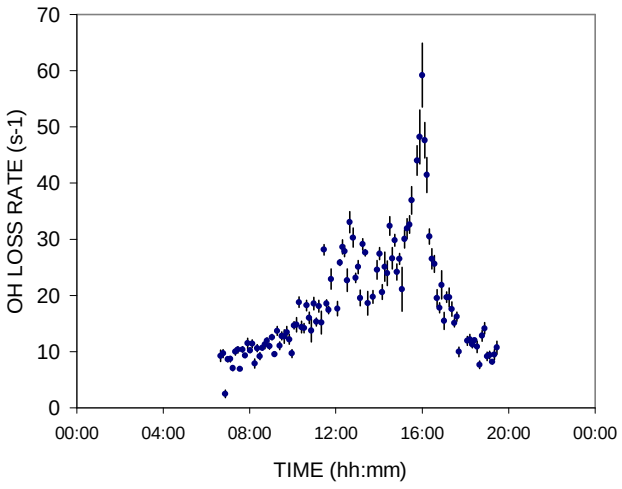

Fig. 5. An example of field measurement data of the OH reactivity from the OP-3 campaign held at Bukit Atur, Borneo on 27 April 2008. The error bars represent the 1 sigma statistical error from linear-least squares fits to individual OH decays.

10 ppbv during the daytime). Measurements were performed from the 12th–29th April, and data were generally taken between dawn and dusk, although a number of night-time measurements were also made. Figure 5 shows an example of a typical dawn until dusk time-series of the measured OH reactivity, exhibiting a distinct diurnal cycle that closely followed that of isoprene. The largest OH reactivity ca. 60 s^{-1}) was recorded after solar noon when the maximum isoprene concentration was observed, and is similar to the value measured by Sinha et. al.(2008) in a tropical rainforest in Suriname. A full interpretation of these data together with model comparisons is underway, and will be reported in a future publication.

5 Conclusions

A flow-tube laser-induced fluorescence instrument has been developed to measure the OH reactivity in the atmosphere and deployed in several field campaigns. The performance of the instrument was fully characterised in the laboratory. A disadvantage of the method, common to other instruments of this type, is the co-production of HO_2 radicals in the sliding injector used to generate OH, and at elevated levels of NO, a correction for production of OH via the reaction of HO_2 with NO is required. However, with knowledge of [HO_2]/[OH] at each position in the flowtube where the decay of OH is measured, and also [NO], the recycling of OH from this reaction can be taken into account analytically. The instrument has been operated in low and high NO_x environments, with measurements taken in a tropical rainforest showing a distinct diurnal profile with OH reactivities reaching as high as $\sim$60 s^{-1}.

Acknowledgements. We are grateful to the Natural Environment Research Council for funding this work (grants NER/B/S/2002/00319, NE/D004756/1 and NE/D002192/1). We are also grateful to the University of Leeds mechanical and electronic workshops, to S. C. Smith, J. A. Davey, C. Moore and A. Moore for technical assistance, and to M. J. Pilling and W. J. Bloss for helpful discussions.

Edited by: M. D. Andrés Hernóndez

References

Atkinson, R.: Kinetics of the gas-phase reactions of OH radicals with alkanes and cycloalkanes, Atmos. Chem. Phys., 3, 2233–2307, 2003, http://www.atmos-chem-phys.net/3/2233/2003/.

Bell, N., Heard, D. E., Pilling, M. J., and Tomlin, A. S.: Atmospheric lifetime as a probe of radical chemistry in the boundary layer, Atmos. Environ., 37, 2193–2205, 2003.

Bloss, W. J., Gravestock, T. J., Heard, D. E., Ingham, T., Johnson, G. P., and Lee, J. D.: Application of a compact all solid-state laser system to the in situ detection of atmospheric OH, HO_2, NO and IO by laser-induced fluorescence, J. Environ. Monitor., 5, 21–28, 2003.

Calpini, B., Jeanneret, F., Bourqui, M., Clapier, A., Vajtai, R., van der Bergh, H.: Direct measurement of the total reaction rate of OH in the atmosphere, Analysis, 27, 328–336, 1999.

Carslaw, N., Creasey, D. J., Heard, D. E., Lewis, A. C., McQuaid, J. B., Pilling, M. J., Monks, P. S., Bandy, B. J., and Penkett, S. A.: Modeling OH, HO_2, and RO_2 radicals in the marine boundary layer 1, Model construction and comparison with field measurements, J. Geophys. Res., 104(D23), 30241–30255, 1999.

Curtis, A. R. and Sweetenham, W. P.: FACSIMILE release H, users manual AERA Report R12805 (HMSO), London, 1987.

Di Carlo, P., Brune, W. H., Martinez, M., Harder, H., Lesher, R., Ren, X. R., Thornberry, T., Carroll, M. A., Young, V., Shepson, P. B., Riemer, D., Apel, E., and Campbell, C.: Missing OH reactivity in a forest: Evidence for unknown reactive biogenic VOCs, Science, 304, 722–725, 2004.

Emmerson, K. M., Carslaw, N., Carslaw, D. C., Lee, J. D., McFiggans, G., Bloss, W. J., Gravestock, T., Heard, D. E., Hopkins, J., Ingham, T., Pilling, M. J., Smith, S. C., Jacob, M., and Monks, P. S.: Free radical modelling studies during the UK TORCH Campaign in Summer 2003, Atmos. Chem. Phys., 7, 167–181, 2007, http://www.atmos-chem-phys.net/7/167/2007/.

Heard, D. E. and Pilling, M. J.: Measurement of OH and HO_2 in the troposphere, Chem. Rev., 103, 5163–5198, 2003.

Jenkin, M. E., Saunders, S. M., Wagner, V., and Pilling, M. J.: Protocol for the development of the Master Chemical Mechanism, MCM v3 (Part B): tropospheric degradation of aromatic volatile organic compounds, Atmos. Chem. Phys., 3, 181–193, 2003, http://www.atmos-chem-phys.net/3/181/2003/.

Johnson, G. P.: Measurements of Tropospheric Radical Concentrations by Laser Induced Fluorescence, Ph. D. Thesis, University of Leeds, 2004.

Kovacs, T. A. and Brune, W. H.: Total OH Loss Rate Measurement, J. Atmos. Chem., 39, 105–122, 2001.

Kovacs, T. A., Brune, W. H., Harder, H., Martinez, M., Simpas, J. B., Frost, G. J., Williams, E., Jobson, T., Stroud, C., Young,

V., Fried, A., and Wert, B.: Direct Measurements of Urban OH Reactivity during Nashville SOS in Summer 1999, J. Environ. Monitor., 5, 68–74, 2003.

Lee, J. D., Smith, S. C., Davey, J. et al.: Measurement of OH Reactivity in the TORCH-2 Campaign, Atmos. Chem. Phys., is going to be submitted, 2009.

Lelieveld, J., Butler, T. M., Crowley, J. N., Dillon, T. J., Fischer, H., Ganzeveld, L., Harder, H., Lawrence, M. G., Martinez, M., Taraborrelli, D., and Williams, J.: Atmospheric oxidation capacity sustained by a tropical forest, Nature, 452, 737–740, 2008.

Lewis, A. C., Carslaw, N., Marriott, P. J., Kinghorn, R. M., Morrison, P., Lee, A. L., Bartle, K. D., and Pilling, M. J.: A larger pool of ozone-forming carbon compounds in urban atmospheres, Nature, 405, 778–781, 2000.

Lewis, A. C., Hopkins, J. R., Carpenter, L. J., Stanton, J., Read, K. A., and Pilling, M. J.: Sources and sinks of acetone, methanol, and acetaldehyde in North Atlantic marine air, Atmos. Chem. Phys., 5, 1963–1974, 2005, http://www.atmos-chem-phys.net/5/1963/2005/.

Li, S., Matthews, J., and Sinha, A.: Atmospheric Hydroxyl Radical Production from Electronically Excited NO_2 and H_2O, Science, 319, 1657–1660, 2008.

Mao, J., Ren, X., Brune, W. H., Olson, J. R., Crawford, J. H., Fried, A., Huey, L. G., Cohen, R. C., Heikes, B., Singh, H. B., Blake, D. R., Sachse, G. W., Diskin, G. S., Hall, S. R., and Shetter, R. E.: Airborne measurement of OH reactivity during INTEX-B, Atmos. Chem. Phys., 9, 163–173, 2009, http://www.atmos-chem-phys.net/9/163/2009/.

Martinez, M., Harder, H., Kovacs, T. A., Simpas, J. B., Bassis, J., Lesher, R., Brune, W. H., Frost, G. J., Williams, E., Stroud, C., Jobson, T., Roberts, J. M., Hall, S. R., Shetter, R. E., Wert, B., Fried, A., Alicke, B., Stutz, J., Young, V. L., White, A. B., and Zamora, R. J.: OH and HO_2 Concentrations, Sources, and Loss Rate during the Southern Oxidants Study in Nashville, Tennessee, Summer 1999, J. Geophys. Res., 108(D19), 4617, doi:10.1029/2003JD003551, 2003.

McKeen, S. A., Mount, G. H., Eisele, F. L., Williams, E., Harder, J., Goldan, P., Kuster, W., Liu, S. C., Baumann, K., Tanner, D., Fried, A., Sewell, S., Cantrell, C., and Shetter, R.: Photochemical modeling of hydroxyl and its relationship to other species during the Tropospheric OH Photochemistry Experiment, J. Geophys. Res., 102(D5), 6467–6493, 1997.

Ren, X., Harder, H., Martinez, M., Lesher, R. L., Oliger, A., Shirley, T., Adams, J., Simpas, J. B., and Brune, W. H.: HO_x Concentrations and OH Reactivity Observations in New York City during PMTACS-NY2001, Atmos. Environ., 37, 3627–3637, 2003.

Ren, X., Brune, W. H., Cantrell, C. A., Edwardss, G. D., Shirley, T., Metcalf, A. R., and Lesher, R. L.: Hydroxyl and Peroxy Radical Chemistry in a Rural Area of Central Pennsylvania: Observations and Model Comparisons, J. Atmos. Chem., 52, 231–257, 2005.

Ren, X., Brune, W. H., Mao, J., Mitchell, M. J., Lesher, R. L., Simpas, J. B., Metcalf, A. R., Schwab, J. J., Cai, C., Li, Y., Demerjian, K. L., Felton, H. D., Boynton, G., Adams, A., Perry, J., He, Y., Zhou, X., and Hou, J.: Behaviour of OH and HO_2 in the winter atmosphere in New York City, Atmos. Environ., 40, 252–263, 2006a.

Ren, X., Brune, W. H., Oliger, A., Metcalf, A. R., Lesher, R. L., Simpas, J. B., Shirley, T., Schwab, J. J., Bai, C., Roychowdhury, U., Li, Y., Cai, C., Demerjian, K. L., He, Y., Zhou, X., Gao, H., and Hou, J.: OH, HO_2, and OH reactivity during the PMTACS-NY Whiteface Mountain 2002 campaign: Observations and model comparison, J. Geophys. Res., 111, D10S03, doi:10.1029/2005JD006126, 2006b.

Sadanaga, Y., Yoshino, A., Watanabe, K., Yoshioka, A., Wakazono, Y., Kanaya, Y., and Kajii, Y.: Development of a Measurement System of OH Reactivity in the Atmosphere by using Laser-Induced Pump and Probe Technique, Rev. Sci. Instrum., 75(3), 2648–2655, 2004a.

Sadanaga, Y., Yoshino, A., Kato, S., Yoshioka, A., Watanabe, K., Miyakawa, Y., Hayashi, I., Ichikawa, M., Matsumoto, J., Nishiyama, A., Akiyama, N., Kanaya, Y., and Kajii, Y.: The importance of NO_2 and volatile organic compounds in the urban air from the viewpoint of the OH reactivity, Geophys. Res. Lett., 31, L08102, doi:10.1029/2004GL019661, 2004b.

Sadanaga, Y., Yoshino, A., Kato, S., and Kajii, Y.: Measurements of OH reactivity and photochemical ozone production in the urban atmosphere, Environ. Sci. Technol., 39, 8847–8852, 2005.

Sander, S. P., Friedl, R. R., DeMore, W. B., Golden, D. M., Kurylo, M. J., Huie, R. E., Orkin, V. L., Moortgat, G. K., Ravishankara, A. R., Kolb, C. E., Molina, M. J., and Finlayson-Pitts, B. J.: Chemical Kinetics and Photochemical Data for use in Atmospheric Studies, Evaluation 14, JPL Publication 02–25, 2002.

Saunders, S. M., Jenkin, M. E., Derwent, R. G., and Pilling, M. J.: Protocol for the development of the Master Chemical Mechanism, MCM v3 (Part A): tropospheric degradation of non-aromatic volatile organic compounds, Atmos. Chem. Phys., 3, 161–180, 2003, http://www.atmos-chem-phys.net/3/161/2003/.

Schultz, M., Heitlinger, M., Mihelcic, D., and Volz-Thomas, A.: Calibration source for peroxy radicals with built-in actinometry using H_2O and O_2 photolysis at 185 nm, J. Geophys. Res.-Atmos., 100(D9), 18811–18816, 1995.

Shirley, T. R., Brune, W. H., Ren, X., Mao, J., Lesher, R., Cardenas, B., Volkamer, R., Molina, L. T., Molina, M. J., Lamb, B., Velasco, E., Jobson, T., and Alexander, M.: Atmospheric oxidation in the Mexico City Metropolitan Area (MCMA) during April 2003, Atmos. Chem. Phys., 6, 2753–2765, 2006, http://www.atmos-chem-phys.net/6/2753/2006/.

Sinha, V., Williams, J., Crowley, J. N., and Lelieveld, J.: The Comparative Reactivity Method - a new tool to measure total OH Reactivity in ambient air, Atmos. Chem. Phys., 8, 2213–2227, 2008, http://www.atmos-chem-phys.net/8/2213/2008/.

Yoshino, A., Sadanaga, Y., Watanabe, K., Kato, S., Miyakawa, Y., Matsumoto, J., and Kajii, Y.: Measurement of Total OH Reactivity by Laser-induced Pump and Probe Technique – Comprehensive Observations in the Urban Atmosphere of Tokyo, Atmos. Environ., 40, 7869–7881, 2006.